COSMO-SkyMed Spotlight Interferometry Over Rural Areas: The Slumgullion Landslide in Colorado, USA

Pietro Milillo, *Student Member, IEEE*, Eric J. Fielding, William H. Shulz, Brent Delbridge, and Roland Bürgmann

***Abstract*—In the last 7 years, spaceborne synthetic aperture radar (SAR) data with resolution of better than a meter acquired by satellites in spotlight mode offered an unprecedented improvement in SAR interferometry (InSAR). Most attention has been focused on monitoring urban areas and man-made infrastructure exploiting geometric accuracy, stability, and phase fidelity of the spotlight mode. In this paper, we explore the potential application of the COSMO-SkyMed® Spotlight mode to rural areas where decorrelation is substantial and rapidly increases with time. We focus on the rapid repeat times of as short as one day possible with the COSMO-SkyMed® constellation. We further present a qualitative analysis of spotlight interferometry over the Slumgullion landslide in southwest Colorado, which moves at rates of more than 1 cm/day.**

***Index Terms*—COSMO-SkyMed (CSK), landslide, SAR interferometry (InSAR), spotlight interferometry.**

I. Introduction

THE ITALIAN COSMO-SkyMed® (CSK) constellation consists of four low-Earth-orbit mid-sized satellites, each equipped with a multimode high-resolution SAR operating at X-band (3.1 cm radar wavelength). The first satellite of the constellation was launched in June 2007 and the last in November 2010. CSK satellites 2 and 3 (COSMO2 and 3) are currently in a tandem-like configuration [Fig. 1(a)]; i.e., with a 1-day time interval between acquisitions. While each satellite has a 16-day repeat interval, the four satellites combined allow for acquisition of up to four images from a given track every 16 days. The tandem-like configuration achieves interferometric acquisitions spanning 24 h by phasing the COSMO3 satellite 112.5° from the regular 90° phase for four satellites [see Fig. 1(b)].

Spotlight SAR is an advanced operation mode that involves sweeping the azimuth beam from forward to backward during imaging to increase the resolution in the azimuth direction by increasing the azimuth bandwidth. The InSAR analysis method exploits the phase difference between two or more coherent complex-valued images to derive path-length differences, generally caused by surface motion, with subcentimetric accuracy. We combine Spotlight SAR with InSAR analyses to measure the surface motion of a landslide at very high-spatial resolution. Such an approach previously has been exploited for monitoring man-made structures and natural disasters [1]–[3]. In the following, we present the details of the data and results of our analysis of images acquired over an active landslide in a rural area of Colorado with particular emphasis on the way a constellation of SAR satellites can monitor surface deformation. The subject landslide (Slumgullion) persistently moves in the order of 1 cm/day, thus providing an ideal setting for such deformation monitoring.

CSK is the largest Italian investment in space systems for Earth observation, commissioned and funded by the Italian Space Agency (ASI) and the Italian Ministry of Defense (MoD) [4]–[6]. The short X-band SAR radar wavelength utilized by the CSK satellites (3.1 cm) allows for a finer resolution and sampling rate of ground displacements than longer wavelength systems (e.g., 6 cm for C-band, 24 cm for L-band); however, these signals are very sensitive to changes in soil moisture and surface roughness. These sensitivities can cause temporal decorrelation of the images and limit the application of X-band interferometry in rural areas. The CSK constellation allows a variety of short time intervals for interferometric pairs (see Table I), which can mitigate the temporal decorrelation. The period for interferometric repeat acquisitions is 16 days with a single satellite. Considering the whole constellation, the current interferometric time period between two successive acquisitions can be much shorter as shown in Table I and Fig. 1(b). SAR spotlight mode relies on the idea that increasing the illuminating time on a target increases the synthetic aperture time, and thus improves the azimuth resolution. In spotlight SAR mode, the antenna is rotated throughout the acquisition from forward to backward.

Beam sweeping can be performed mechanically by rotating the satellite or by steering a phased-array antenna electronically.

Manuscript received December 19, 2013; revised July 28, 2014; accepted August 01, 2014. Date of current version August 21, 2014. Original COSMO-SkyMed data are copyright 2010–2013 by the Italian Space Agency and was provided under CSK AO PI project 2237 and under the JPL-ASI CIDOT Dynamic Processes project. This work was supported in part by the NASA Earth Surface and Interior focus area and performed at the Jet Propulsion Laboratory, California Institute of Technology. The work of P. Milillo was done while he was a Visiting Student Researcher at Caltech. Any use of trade, product, or firm names is for descriptive purposes only and does not imply endorsement by the U.S. Government.

P. Milillo is with the School of Engineering, University of Basilicata, 85100 Potenza, Italy (e-mail: pietro.milillo@unibas.it).

E. J. Fielding is with the Jet Propulsion Laboratory, California Institute of Technology, Pasadena, CA 91109, USA.

W. H. Shulz is with United States Geological Survey, Denver, CO 80225, USA.

B. Delbridge and R. Bürgmann are with the Department of Earth and Planetary Science, University of California, Berkeley, CA 94720, USA.

Color versions of one or more of the figures in this paper are available online at http://ieeexplore.ieee.org.

Digital Object Identifier 10.1109/JSTARS.2014.2345664

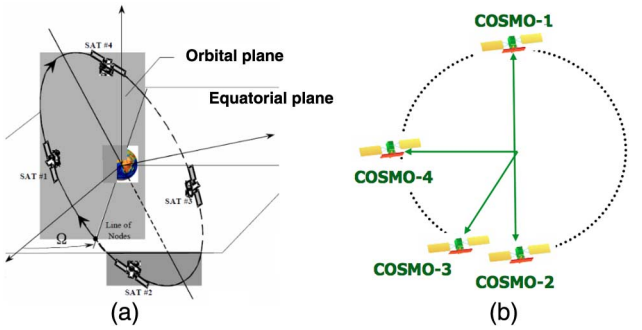

Fig. 1. (a) CSK orbital plane (adapted from [6]). (b) Present CSK satellite positions in the orbital plane.

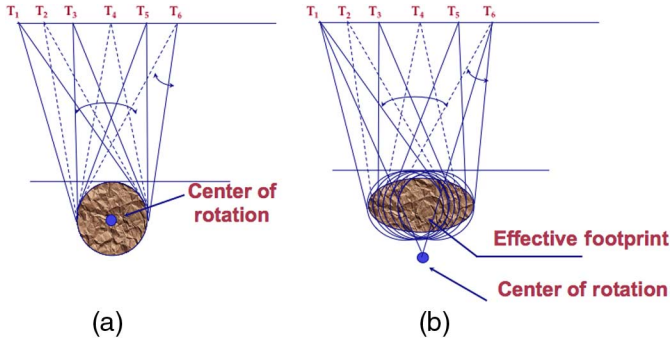

Fig. 2. Virtual rotation center in (a) staring spotlight mode (left) and (b) sliding spotlight mode (right) (from [5]).

TABLE I
TIME PERIOD BETWEEN TWO SUCCESSIVE POSSIBLE INTERFEROMETRIC ACQUISITIONS OVER THE SAME TARGET

		Clockwise →			
	$\Delta T_{(days)}$	CSK1	CSK2	CSK3	CSK4
Counter clockwise ↓	CSK1	16	8	9	12
	CSK2	8	16	1	4
	CSK3	7	15	16	3
	CSK4	4	12	13	16

Clockwise directions are related to Fig. 1(b).

The major drawback is that having the azimuth beam pointing at the same area for a longer period of time limits the extent of the illuminated area in azimuth.

Modern SAR systems like CSK and TerraSAR-X are examples of phased-array systems, while the Indian and Israeli satellites RISAT-2 and Tec-SAT [7], [8] are examples of mechanically steered spotlight SAR. The CSK system uses a sliding spotlight mode, which can image a larger area than the more concentrated staring spotlight mode that has the rotation center inside the scene [Fig. 2(a)]. The sliding spotlight mode can be described as using a virtual rotation center, which is further away from the radar than the imaging scene [Fig. 2(b)]. The azimuth antenna pattern of spotlight is then [9]

$$G = G_0 \sin c^2 \left[\frac{L}{\lambda} \left(\frac{V_s \tau}{R_0} - k\tau \right) \right]$$

$$= G_0 \sin c^2 \left[\frac{L}{\lambda} \frac{V_s \tau}{R_0} \left(1 - \frac{R_0 k}{V_s} \right) \right] \quad (1)$$

$$= G_0 \sin c^2 \left[\frac{L}{\lambda} \frac{V_s \tau}{R_0} \left(1 - \frac{R_0 k}{V_s} \right) \right] \quad (2)$$

where G_0 is the antenna gain at closest approach, L is the azimuth antenna size, λ is the wavelength, and τ is the azimuth (along-track) time. V_s is the sensor velocity, R_0 is the closest distance between the sensor and the target, and k is the antenna rotation rate. From (2), it can be seen that spotlight SAR can be considered as an effective strip-map SAR with a fixed antenna size $Lc = \alpha L$, where α is the shrinking factor [9] and can be described as

$$\alpha = 1 - \frac{R_0 k}{V_s}. \quad (3)$$

The azimuth resolution of spotlight SAR can be approximately written as α L/2. That is, the spotlight SAR can obtain better (smaller) azimuth resolution than strip-map SAR by a factor of α. CSK has one civilian spotlight mode called enhanced Spotlight mode S2, which is a sliding spotlight mode. This mode is characterized by range-azimuth coverage of 11 × 11 km with pulse repetition frequency (PRF) values that vary in the range of 3148.1–4116.7 Hz [5]. Chirp length is about 70–80 ms with a range bandwidth of 185.2 MHz–400 MHz. The α value for the CSK-enhanced Spotlight S2 mode is about 1/3.

II. CASE STUDY: THE SLUMGULLION LANDSLIDE

Landslides are considerable natural hazards and present substantial risk to the built environment and human life. Hence, studying landslide phenomena is important for improving the understanding of the mechanisms of landslide motion. Recent studies have utilized remote-sensing data including automatic detection of slowly moving landslides using InSAR products [30], a joint approach using DInSAR, LIDAR, and archival air photos to quantify landsliding and sediment transport [31], and persistent scatterer techniques for monitoring landslides in large regions [33]. Results of such studies potentially lead to fundamental advances in our knowledge of the spatiotemporal patterns of landslide motion in response to changes in environmental parameters such as rainfall, snowmelt, and atmospheric pressure.

Resolving the kinematics of landslides is a prerequisite to evaluate potential controls on motion. Generally, the displacement of a given landslide is measured at only a few locations using *in situ* sensors or surveying (e.g., GPS, LIDAR) techniques. However, because complex landslides consist of multiple kinematic elements or units whose relative motion accommodates deformation within the slide, point measurements are oftentimes insufficient for such evaluations and may even be misleading. Additionally, the interplay between kinematic elements comprising landslides strongly controls their motion, so widespread measurements of the complete surface displacement field are most useful but rarely obtained. This is often due to technological deficiencies in ground-based monitoring instrumentation, inaccessibility of hazardous landslide areas, insufficient displacement to resolve using standard mapping and monitoring techniques, and the extensive labor

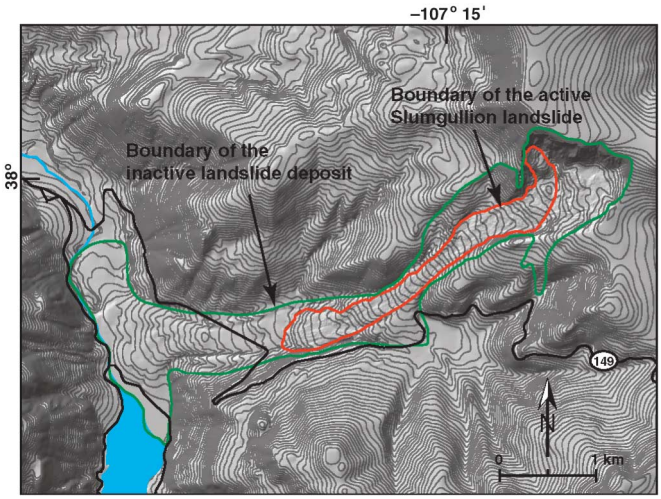

Fig. 3. Shaded relief map of the Slumgullion landslide. Relief and topographic contours (10 m interval) derived from USGS National Elevation Dataset.

required. InSAR has the ability to reveal landslide-wide kinematics on the timescale of days or weeks for faster moving landslides, to resolve fine temporal variations in kinematics, and thus provide data necessary to fully evaluate controls on landslide motion when used in conjunction with *in situ* observations of environmental and groundwater conditions and appropriate laboratory tests of landslide material properties.

We studied the Slumgullion landslide located in the San Juan Mountains of southwestern Colorado (Fig. 3), because it is a perfect test site for emphasizing the importance of having a finer resolution and a short repeat acquisition time in order to detect and characterize large deformation gradients that would be aliased with a single X-band satellite configuration. The Slumgullion landslide occurs in deeply weathered tertiary volcanic rocks and consists of a younger, active upper part that moves on and over an older, larger, inactive part. The active landslide (Fig. 3) is about 3.9 km long, averages about 300 m wide and 14 m deep, and has an estimated volume of 20×106 m^3 [29].

The slide has an average ground-surface inclination of 8° and extends through alpine and subalpine ecological zones [22] with spruce and aspen tree cover. The landslide moves persistently throughout the year at average rates of 0.1–2.0 cm/day; acceleration to about twice the average speed occurs during spring snowmelt and prolonged rainy periods when elevated pore-water pressures result in decreased frictional strength [23], [27]. Shear-zone dilation and consequent pore-water pressure decrease appear to retard acceleration [20], [23], while the onset of low-atmospheric tides appears to trigger daily acceleration episodes [24].

Detailed structural mapping [19] during the early 1990s and displacement measurements of hundreds of points on the landslide surface from aerial photographs taken during 1985 and 1990 [26] reveal that multiple kinematic elements accommodate differential displacement within the landslide. Differential internal displacement and strike-slip displacement along the landslide's marginal boundaries primarily occur along well-developed faults and fractures. Terrestrial InSAR surveys during 2010 indicated that the kinematic elements have remained spatially consistent with those identified from the 1990s studies, but that elements at the upper part of the landslide have slowed significantly [25]. This slowing may be due to reduced precipitation [17]. The spatial stability of the kinematic elements suggests that landslide boundary geometry controls their occurrence and character [10], [16], [19]. Slumgullion's continuous but temporally and spatially variable movement at moderate (for landslides) rates of around 1 cm/day (up to 500 times faster than the Berkeley Hills landslides [28]) and accessibility make it a perfect natural laboratory for studying the mechanisms of landslide motion.

CSK Spotlight interferometry appears very promising for advancing the understanding of the mechanisms that control the rate of movement of landslides and for measuring the spatial distribution of displacements across the Slumgullion landslide. Combining these spatial observations with the detailed temporal measurements made at the monitoring site may lead to the formulation of a complete model for the motion of the landslide that can be generalized to other landslides around the world.

TABLE II
INTERFEROGRAMS SHOWN IN THIS REPORT

Processed interferograms

Dates (Master–Slave)		Bperp (m)	Beam	Incidence angle
2010-05-13	2010-05-12	24.03	Ascending 20	48°
2012-03-27	2012-03-26	6.43	Descending 20	48°
2012-05-18	2012-05-17	–127.13	Ascending 20	48°
2012-06-03	2012-06-02	–244.45	Ascending 20	48°
2013-07-31	2013-07-30	141.53	Descending 13	40°
2013-08-25	2013-08-24	155.66	Ascending 20	48°
2013-09-26	2013-09-25	148.19	Ascending 20	48°

Bperp is the perpendicular component of baseline in meters. Incidence angle measured from the vertical.

III. DATASET USED AND ACQUISITIONS STRATEGY

The dataset consists of three interferometric stacks (one in ascending and two in descending geometry) of CSK-enhanced Spotlight S2 data acquired starting in 2010. We processed a total of 16 SAR scenes that are divided in three datasets with right look direction and incidence angles of 48° for both ascending (satellite moving north and looking east) and descending (satellite moving south and looking west) geometry and 40° for only descending geometry. Polarization is HH (horizontal transmit and receive). Table II shows the datasets used for our analysis.

The acquisitions were planned to avoid acquiring data during the winter since the area typically is covered by snow then, and no useful signal of landslide motion can be recorded. The yearly campaign time span is April–September and so far covers 4 years starting from May 2010.

Fig. 4 shows the baseline distribution for the three tracks of CSK data over Slumgullion. We selected a subset of eight 1-day pairs and one 4-day pair that have short spatial baselines for analysis in this study (marked in red in Fig. 4).

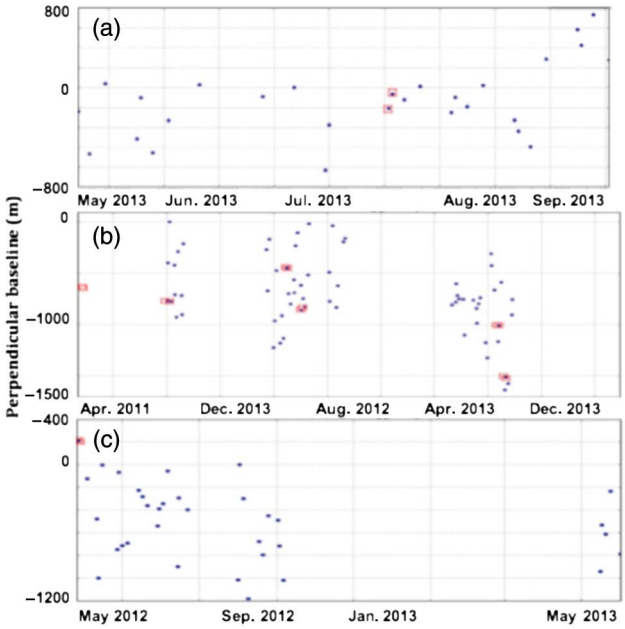

Fig. 4. Baseline (perpendicular component) plots for the three datasets. Red boxes enclose the 1-day pairs analyzed in this work, most of which are too closely spaced to be visible as separate dots here. (a) Descending geometry, angle 40°. (b) Ascending geometry, angle 48°. (c) Descending geometry, angle 48°.

IV. Results

We start with the standard single-look complex (SLC) images processed by the Italian Space Agency and provided in a zero-Doppler geometry. We then use the JPL/Caltech SAR interferometry package InSAR Scientific Computing Environment (ISCE) developed at JPL and Stanford to perform the rest of the InSAR processing [11]. We developed and adapted parts of ISCE in order to support CSK Spotlight interferometry. We use the USGS National Elevation Dataset 1/3-arcsecond (roughly 10 m posting) digital elevation model to calculate and remove the topographic phase, and for geocoding the final interferograms. Phase unwrapping relies on the SNAPHU program [15] with the minimum cost flow and smooth options. The unwrapped phase is converted to range change in the radar line-of-sight direction with the radar wavelength.

Fig. 5 shows the differential interferograms processed with ISCE for five 1-day pairs on the ascending track. In this SAR geometry, the landslide motion that is to the west with a small vertical component is moving toward the COSMO satellites, which is shown as positive motion. Fig. 6 shows the differential interferograms for the descending tracks, with one for each of the two beams (incidence angles). In the descending SAR geometry, the landslide motion is away from the satellites resulting in negative values. Note that some of the interferograms [especially, Fig. 5(c)–(e)] have significant changes in the vertical distribution of atmospheric water vapor between the two dates that causes the InSAR phase to be correlated with elevation. The interferograms with long spatial perpendicular baselines [Fig. 5(b)–(d), 6(a); see also Table II] have some phases caused by topographic residuals in the lower inactive

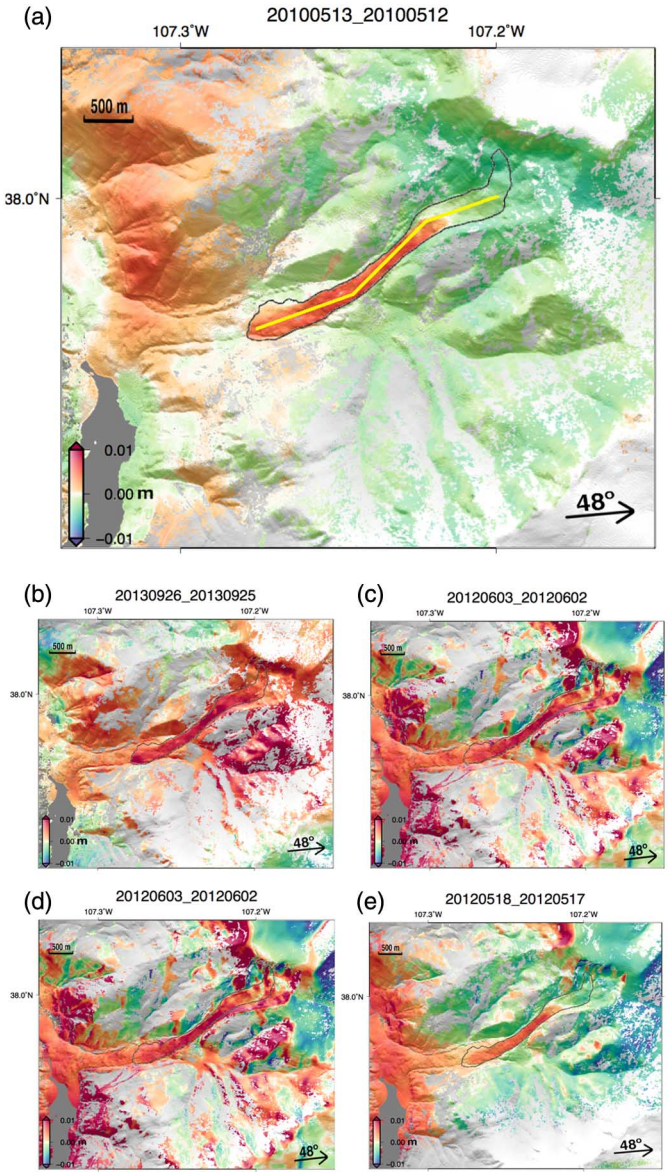

Fig. 5. Five 1-day unwrapped and geocoded interferograms from the ascending track of CSK Spotlight mode images for the Slumgullion landslide. Color scale is same on all plots. The orange and red colors show the rapidly moving active part of the landslide (∼1 cm horizontal motion during the 1-day observation period), which is moving toward the satellite on the ascending tracks. Blue and green colors are moving slowly or not moving. The black line marks the boundary of the active landslide based on field observations. Yellow line on (a) is line of profiles shown in Fig. 7. Data acquired during the summer likely are noisier than those from other periods due to changes in soil moisture from intense rainfall. (a) May 12–13, 2010 incidence, (b) September 25–26, 2013, (c) June 2–3, 2012, (d) August 24–25, 2013, and (e) May 17–18, 2012.

part of the landslide where the steep sides of the landslide are not adequately represented in the DEM.

Estimated motion of the Slumgullion landslide varies considerably between the dates of the interferograms shown in Figs. 5 and 6, with the 1-day pairs providing a series of snapshots of the landslide motion over single days. Profiles of the interferograms approximately along the center of the landslide are shown in Fig. 7. On some days, we can see faster motion at the narrow

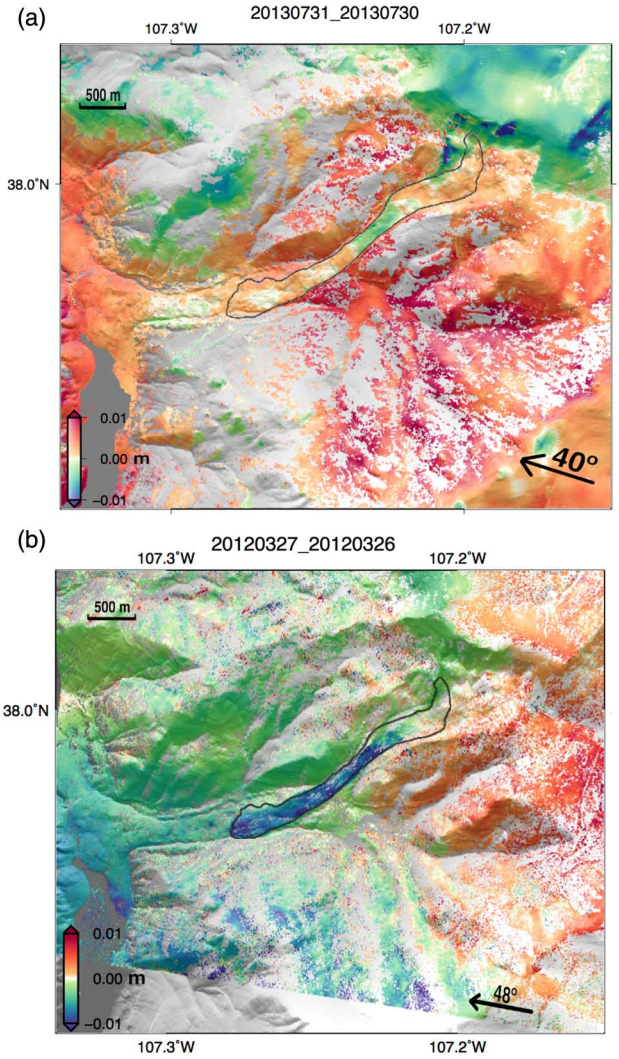

Fig. 6. One-day unwrapped and geocoded interferogram from descending tracks of CSK Spotlight mode images for the Slumgullion landslide. (a) July 30–31, 2013 beam 13, incidence angle 40°. (b) March 26–27, 2012 beam 20, incidence angle 48°. The green and blue colors show the rapidly moving active part of the landslide (∼1 cm horizontal motion during the 1-day observation period), which is moving away from the satellite on the descending tracks. Orange and red colors are moving slowly or not moving. Black outline shows the active portion of the landslide based on field observations.

"neck" of the landslide [Figs. 5(b)–(d) and 6(a)], and on other days [Figs. 5(a), (e), and 6(b)], the landslide motion is more uniform from the neck area to the toe of the active landslide. This sampling is not complete, but we note that the days in the spring have more uniform motion than the days later in the summer and early fall. Additional analysis will be needed to confirm whether this is generally true. Interferograms from the summer months are less coherent than in the spring, likely due to the large changes in soil moisture from intense rainfall and leaves on deciduous trees.

Fig. 8 shows two 4-day interferograms from the same time interval, 21–25 August 2012, from both ascending (east-looking) and descending (west-looking) tracks. Over this longer time interval, phase unwrapping is more difficult as discussed below, and we show only the wrapped interferograms.

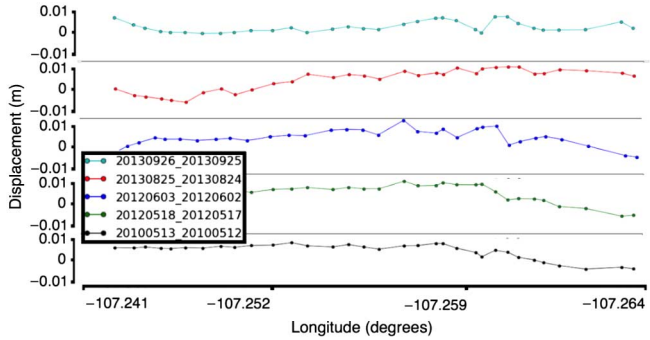

Fig. 7. Profiles of line-of-sight displacements from the ascending interferograms shown in Fig. 5, along the line in Fig. 5(a), plotted as a function of longitude with the toe of the landslide to the left. Two spring interferograms (bottom two) have high velocity extending to the toe, while summer and fall interferograms mostly show decrease velocity toward toe.

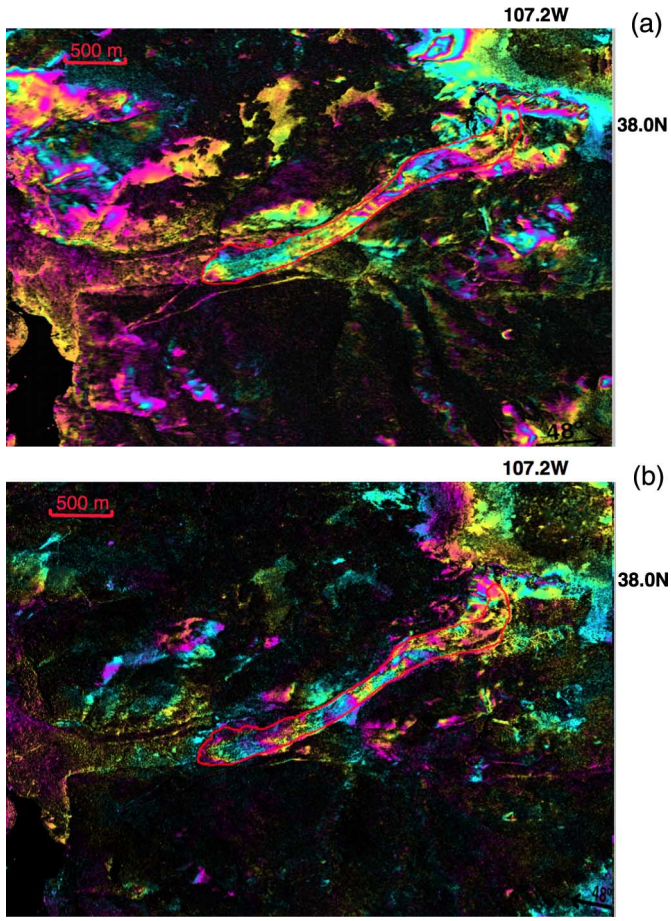

Fig. 8. Four-day wrapped interferograms from 21 August to 25 August 2012 pair of CSK Spotlight mode images for the lower part of the Slumgullion landslide. (a) Ascending-track and (b) descending-track. Wrapped phase (2π radians equals 1.55 cm) is combined with the radar amplitude. Across the edges in the middle of the slide, there was 5–6 cm of motion or about two fringes at the X-band radar wavelength. Fringes within the slide show differences in velocity between the kinematic units. These interferograms have been geocoded.

Over longer time intervals, the Slumgullion landslide moves many meters so InSAR measurements are not possible. We use another method called pixel-offset tracking or sub-pixel correlation to measure the motion over a 1-year time

interval (e.g., [33], [34]). Pixel-offsets measure displacements in both the slant range (line-of-sight) direction that is the same as the InSAR measurements and horizontally in the azimuth or along-track direction. Typically, the pixel-offset measurements can be made to 1/10 or 1/20 of the image pixel size, which is 50 cm in azimuth and 70 cm in range for these CSK Spotlight images. The range displacements over a year are over 3 m and azimuth (southward) displacements over 2.5 m in the fastest moving portion. The pixel-offset measurements in two dimensions from ascending and descending tracks can be combined to estimate the full three-dimensional (3-D) surface motion, if the time intervals are similar.

V. Discussion and Future Work

CSK radar operates in X-band with a wavelength of about 3.1 cm. The short radar wavelength gives increased sensitivity to ground motion but also causes more rapid loss of coherence with time. The interferograms in Figs. 5–7 have been processed using ISCE with 4 range and 4 azimuth looks (pixels averaged), with a final geocoded pixel spacing of 1.08×10^{-5} degrees or about 1.2 m. The orange areas in Fig. 5 have moved about 8 mm in the radar line of sight, which is eastward at 42° from the vertical for these ascending track interferograms in the 1-day interval. If we assume the displacement is purely horizontal, this corresponds to about 1.2 cm/day of motion of the landslide surface, which is very consistent with the ground measurements [12], [14], [23]. Over this very short time interval, the coherence at X-band is quite high over nearly the entire landslide surface but somewhat lower over dense forests nearby (Fig. 10).

Ground observations show that the landslide moves fastest during and for about 1 month following spring snowmelt, which occurs March–May [14], [23]. The landslide extends from an elevation of 3700 m to an elevation of 3000 m, which results in snowmelt occurring days to weeks earlier on the lower part of the landslide than on the upper part. This variable snowmelt timing should result in acceleration occurring earlier in the lower part of the landslide, and our results support this; interferograms from March to May reveal relatively consistent speed from the landslide neck to the toe, while interferograms from June to September show the landslide neck clearly moving most rapidly, consistent with the distribution of speeds measured along the length of the landslide from 1985 to 1990 [26].

Over time intervals longer than 1 day, the CSK interferograms start to lose the fringes where the ongoing displacement across the strike-slip faults along the edges of the landslide exceeds the X-band InSAR ambiguity (1.5 cm). In the 1-day interferograms (Figs. 5 and 6), the displacement across the edges is less than one fringe, which makes unwrapping straightforward. For longer time-span interferograms such as the 4-day interferogram shown in Fig. 8, phase unwrapping is not so easy. In the middle of the active zone, there is 3–4 cm of line-of-sight motion across the edges of the landslide in 4 days or about 2 fringes at the X-band wavelength of CSK. The fringes within the landslide over the 4-day time interval show that different parts of the landslide are moving at different rates over this time. We will compare these short-term spatial variations with the long-term kinematic unit velocities measured with other techniques to see if the motions change in time and space (Fig. 9).

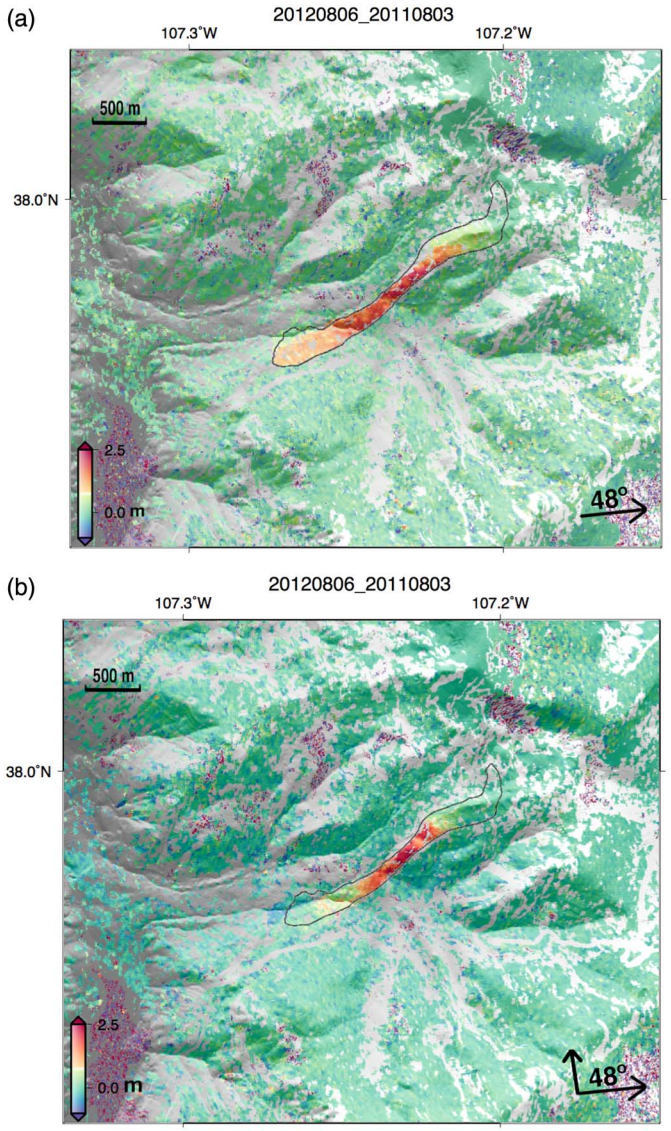

Fig. 9. One-year unwrapped and geocoded pixel tracking offsets field from ascending track of CSK Spotlight mode images for the Slumgullion landslide. (a) Range (line-of-sight). (b) Azimuth (along-track). The red and orange colors show the rapidly moving active part of the landslide (values over 2.5 m have been clipped to better show the moderate motion), which is moving toward the satellite in range and south in azimuth on this ascending track. Green color is moving slowly or not moving. Black outline shows the active portion of the landslide based on field observations.

Future work will include using a mask separating the stationary surroundings from the fast-moving landslide to unwrap these interferograms. The black line in Figs. 5 and 6 shows the boundaries of the active landslide, which could be projected into the radar coordinates and used to prepare a mask. We also plan to explore the application of pixel tracking [14] to the high-resolution SAR images.

The velocity of the landslide at the main monitoring station has shown systematic variations over the year, with the highest speed after the spring snowmelt [14]. To better understand this seasonal variation in the velocity, we are also acquiring NASA

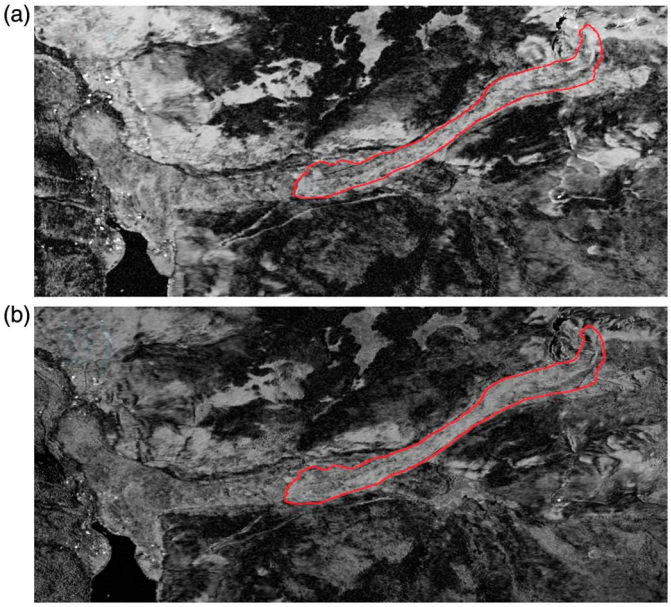

Fig. 10. Coherence maps of (a) 1-day and (b) 4-day interferograms. Coherence at X-band is quite high (light tones) over nearly the entire landslide surface but somewhat lower over dense forests nearby. Area is similar to that shown in Fig. 7, and these coherence maps have been geocoded.

Uninhabited Aerial Vehicle SAR (UAVSAR) datasets at three key times: 1) during the slow season (fall or winter), 2) during the acceleration phase, and 3) during the deceleration phase. We also plan to use the TanDEM-X bistatic (single-pass) coverage of the landslide in late 2011, with the TerraSAR-X and TanDEM-X spacecraft flying in a close tandem configuration a few hundred meters apart or less, to develop higher resolution and more recent digital elevation models. Persistent scatterers time series analysis will be performed in order to exploit 3-D phase unwrapping techniques as well as to enable the analysis of the CSK InSAR pairs with time intervals longer than the 1-day pairs.

ACKNOWLEDGMENT

We thank P. S. Agram for help with adjusting the ISCE software to process the CSK Spotlight mode data. We thank C. Serio for providing support. We thank L. Dini and the ASI CSK ordering staff for their help with the CSK acquisitions.

REFERENCES

[1] F. Covello *et al.*, "One-day interferometry results with the COSMO-SkyMed constellation," in *Proc. IEEE Int. Geosci. Remote Sens. Symp. (IGARSS)*, Jul. 2010, pp. 4397–4400.

[2] D. O. Nitti *et al.*, "Quantitative analysis of stripmap and spotlight SAR interferometry with COSMO-SkyMed constellation," in *Proc. IEEE Int. Geosci. Remote Sens. Symp.*, Jul. 2009, pp. II-925–II-928.

[3] M. Eineder, N. Adam, R. Bamler, F. Nestor Yague-Martinez, and H. Breit, "Spaceborne spotlight SAR interferometry with TerraSAR-X," *IEEE Trans. Geosci. Remote Sens.*, vol. 47, no. 5, pp. 1524–1535, May 2009.

[4] F. Covello *et al.*, "COSMO-SkyMed an existing opportunity for observing the Earth," *J. Geodyn.*, vol. 49, no. 3–4, pp. 171–180, 2010.

[5] Agenzia Spaziale Italiana, *COSMO-SkyMed SAR Products Handbook*. Rome, Italy: ASI, Agenzia Spaziale Italiana, 2007.

[6] A. Coletta *et al.*, "Il programma COSMO-SkyMed: Descrizione della missione e del sistema e primi risultati," *Rivista italiana di telerilevamento*, vol. 40, no. 2, pp. 5–13, 2008.

[7] Sharing Earth Observation Resources, *eOPortal Directory, RISAT-2* [Online]. Available: https://directory.eoportal.org/web/eoportal/satellite-missions/r/risat-2

[8] Y. Sharay and U. Naftaly, "TecSAR satellite -novel approach in space SAR design," in *Proc. Int. Radar Symp. India (IRSI)*, Bangalore, India, Dec. 2005, pp. 20–22.

[9] X. Z. Ren, Y. Qin, and L. H. Qiao, "Interferometric properties and processing for spaceborne spotlight SAR," *Prog. Electromagn. Res. B*, vol. 36, p. 267, 2012.

[10] D. Crandell and D. Varnes, "Movement of the Slumgullion earthflow near Lake City, Colorado," in *Professional Paper 424-B*. U.S. Geological Survey, 1961.

[11] H. A. Zebker, S. Hensley, P. Shanker, and C. Wortham, "Geodetically accurate InSAR data processor," *IEEE Trans. Geosci. Remote Sens.*, vol. 48, no. 12, pp. 4309–4321, Dec. 2010.

[12] B. G. Delbridge, R. Burgmann, E. J. Fielding, S. Hensley, and W. H. Schulz, "Surface flow kinematics derived from airborne UAVSAR interferometric synthetic aperture radar to constrain the physical mechanisms controlling landslide motion," in *Proc. AGU Fall Meeting 2013-G33D-08*, 2013, vol. 1, p. 8.

[13] F. Casu, A. Manconi, A. Pepe, and R. Lanari, "Deformation time-series generation in areas characterized by large displacement dynamics: The SAR amplitude pixel-offset SBAS technique," *IEEE Trans. Geosci. Remote Sens.*, vol. 49, no. 7, pp. 2752–2763, Jul. 2011.

[14] J. Coe *et al.*, "Seasonal movement of the Slumgullion landslide determined from Global Positioning System surveys and field instrumentation, July 1998–March 2002," *Eng. Geol.*, vol. 68, pp. 67–101, 2003.

[15] C. W. Chen and H. A. Zebker, "Phase unwrapping for large SAR interferograms: Statistical segmentation and generalized network models," *IEEE Trans. Geosci. Remote Sens.*, vol. 40, no. 8, pp. 1709–1719, Aug. 2002.

[16] J. A. Coe, J. P. McKenna, J. W. Godt, and R. L. Baum, "Basal-topographic control of stationary ponds on a continuously moving landslide," *Earth Surf. Processes Landforms*, vol. 34, pp. 264–279, 2009.

[17] J. A. Coe, "Regional moisture balance control of landslide motion: Implications for landslide forecasting in a changing climate," *Geology*, vol. 40, no. 4, pp. 323–326, 2012.

[18] D. M. Cruden and D. J. Varnes, "Landslide types and processes," in *Landslides, Investigation and Mitigation, Transportation Research Board Special Report*, A. K. Turner and R. L. Schuster, Eds. Washington, DC, USA: National Research Council, 1996, vol. 247, pp. 36–75.

[19] R. W. Fleming, R. L. Baum, and M. Giardino, *Map and Description of the Active Part of the Slumgullion Landslide, Hinsdale County, Colorado*. U.S. Geological Survey Geologic Investigations Series Map I-2672, 1999, 34pp.

[20] J. S. Gomberg, W. H. Schulz, P. Bodin, and J. W. Kean, "Seismic and geodetic signatures of fault slip at the Slumgullion landslide natural laboratory," *J. Geophys. Res.*, vol. 116, B09404, 2011, doi: 10.1029/2011JB008304.

[21] P. W. Lipman, *Geologic Map of the Lake City Caldera Area, Western San Juan Mountains, Southwestern Colorado*. U.S. Geological Survey Miscellaneous Investigation Series Map I-962, scale 1:48,000, 1976.

[22] D. Love, "Subarctic and subalpine: Where and what?," *Arct. Alp. Res.*, vol. 2, no. 1, pp. 63–73, 1970.

[23] W. H. Schulz, J. P. McKenna, G. Biavati, and J. D. Kibler, "Relations between hydrology and velocity of a continuously moving landslide—Evidence of pore-pressure feedback regulating landslide motion?," *Landslides*, vol. 6, pp. 181–190, 2009.

[24] W. H. Schulz, J. W. Kean, and G. Wang, "Landslide movement in southwest Colorado triggered by atmospheric tides," *Nat. Geosci.*, vol. 2, no. 12, pp. 863–866, 2009.

[25] W. H. Schulz *et al.*, "Kinematics of the Slumgullion landslide revealed by ground-based InSAR surveys," in *Landslides and Engineered Slopes, Protecting Society through Improved Understanding*, E. Eberhardt, C. Froese, A. K. Turner, and S. Leroueil, Eds. New York, NY, USA: Taylor & Francis, 2012, vol. 2, pp. 1273–1279.

[26] W. K. Smith, *Photogrammetric Determination of Movement on the Slumgullion Slide, Hinsdale County, Colorado, 1985–1990*. U.S. Geological Survey Open—File Report 93-597, 1993.

[27] D. J. Varnes and W. Z. Savage, *The Slumgullion Earth Flow: A Large-Scale Natural Laboratory*. U.S. Geological Survey Bulletin 2130, 1996, 95pp.

[28] G. E. Hilley, R. Bürgmann, A. Ferretti, F. Novali, and F. Rocca, "Dynamics of slow-moving landslides from permanent scatterer analysis," *Science*, vol. 304, pp. 1952–1955, 2004.

[29] M. Parise and R. Guzzi, *Volume and Shape of the Active and Inactive Parts of the Slumgullion Landslide, Hinsdale County, Colorado*. U.S. Geological Survey Open—File Report 92-216, 1992, 29 p.
[30] C. Zhao, Z. Lu, Q. Zhang, and J. De la Fuente, "Large-area landslide detection and monitoring with ALOS/PALSAR imagery data over Northern California and Southern Oregon, USA," *Remote Sens. Environ.*, vol. 124, pp. 348–359, 2012.
[31] J. J. Roering, L. L. Stimely, B. H. Mackey, and D. A. Schmidt, "Using DInSAR, airborne LiDAR, and archival air photos to quantify landsliding and sediment transport," *Geophys. Res. Lett.*, vol. 36, 2009.
[32] D. Notti, A. Colombo, C. Meisina, L. Lanteri, and F. Zucca, "Studying and monitoring large landslides with persistent scatterer data," in *Proc. Int. Conf. Vajont 1963–2013*, 2013, p. 30.
[33] A. Singleton, Z. Li, T. Hoey, and J. P. Muller, "Evaluating sub-pixel offset techniques as an alternative to D-InSAR for monitoring episodic landslide movements in vegetated terrain," *Remote Sens. Environ.*, vol. 147, pp. 133–144, 2014.
[34] E. Pathier *et al.*, "Displacement field and slip distribution of the 2005 Kashmir earthquake from SAR imagery," *Geophys. Res. Lett.*, vol. 33, no. 20, p. L20310, 2006, doi: 20310.21029/22006GL027193.

Pietro Milillo (SM'12) was born in Bari, Italy, in 1989. He received the Laurea bachelor degree and the Master degree in physics from the University of Bari, Bari, Italy, in 2012, with a thesis on synthetic aperture radar and GPS data processing. He is currently pursuing the Ph.D. degree at the University of Basilicata, Potenza, Italy.

Since 2013, he is a Visiting Researcher Student with Caltech—Jet Propulsion Laboratory, California Institute of Technology, Pasadena, CA, USA. His research interests include digital signal processing with particular attention to GPS and COSMO-SkyMed (CSK) SAR data analysis, interferogram generation, digital elevation model validation, persistent scatterers, SBAS techniques, remote sensing and Earth processes.

Eric J. Fielding received the A.B. degree in earth sciences from Dartmouth College, Hanover, NH, USA, and the Ph.D. degree in geological sciences from Cornell University, Ithaca, NY, USA.

Since 1994, he has been a Research Scientist with Jet Propulsion Laboratory, California Institute of Technology, Pasadena, CA, USA. He was also a Research Scientist with the University of Oxford, Oxford, U.K., and a Visiting Research Scientist with the University of Cambridge, Cambridge, U.K. His research interests include the application of synthetic aperture radar interferometry to measure deformation in and around faults before, during, and after earthquakes.

Dr. Fielding is a member of the American Geophysical Union, Geological Society of America, and Seismological Society of America.

William H. Shulz, photograph and biography not available at the time of publication.

Brent Delbridge, photograph and biography not available at the time of publication.

Roland Bürgmann, photograph and biography not available at the time of publication.